

Epidemic Processes in Networks: A Comprehensive Study of SIR Model and Network Topologies*

Li Yike and Elena Gubar

*St. Petersburg State University,
Faculty of Applied Mathematics and Control Processes,
7/9, Universitetskaya nab., St. Petersburg, 199034, Russia
E-mail: st102941@student.spbu.ru; e.gubar@spbu.ru*

Abstract In this paper, we explore the dynamics of epidemic processes on different types of single-layer network structures, emphasizing the impact of network structure on the spread of disease. We first propose a single-layer SIR (susceptible-infected-recovered) network model and investigate the impact of network structure on virus transmission. Numerical simulation results indicate that in scale-free networks, infections in hub nodes lead to faster and more widespread spread compared to the absence of such a network. In terms of epidemic control, the importance of disconnecting key nodes is emphasized. In random networks, transmission is generally faster and has higher peak infection levels than in scale-free networks. The findings reveal that network topology and initial infection nodes profoundly influence virus spread patterns, offering critical insights for designing targeted epidemic control strategies that minimize transmission by breaking key network links.

Keywords: SIR network model, epidemic processes, random network.

1. Introduction

In human society, infectious diseases have always been a major global challenge. From smallpox and the plague to cholera, these diseases have claimed countless lives. According to the World Health Organization, seasonal influenza and its complications cause massive deaths annually (Tamerius et al., 2011). Economically, The World Bank similarly estimated that a flu pandemic causing 28 million or more excess deaths could result in a loss of as much as 5% of global GDP (Bloom et al., 2019). Therefore, exploring effective control measures to curb the spread of infectious diseases is of great theoretical and practical significance for epidemic management. The concept and term "epidemiology" can be traced back to Hippocrates. His work "Epidemics" served as a model for many later studies (Payne, 1893). The formation phase of the epidemiology discipline spanned from the late 18th century to the early 20th century, with Daniel Bernoulli's smallpox model in 1760 (Brauer, 2008). Most disease models classify individuals or hosts by disease status. Modern mathematical epidemiology began with the biochemist Kermack and the physician McKendrick's SIR (Susceptible-Infectious-Recovered) model (Kermack et al., 1927). Subsequently, many more complex models were created to simulate epidemic processes, however most were based on the concepts of the SIR model.

*This work was supported by the China Scholarship Council, grant number 202309010305.

Traditional compartmental models assume that individuals interact within fixed compartments and that viruses spread through contact. In contrast, virus transmission models that consider network topologies more realistically simulate human interactions in complex social networks, accounting for connections and transmission paths within different social circles. The traditional epidemic models have been extended to network topologies (Pastor-Satorras et al., 2001a). Barabási et al. focused on the generation mechanisms of scale-free networks, providing an important foundation for understanding virus spread in these networks (Barabási et al., 1999). Pastor-Satorras et al. explored the dynamic behavior and epidemic states on complex networks, analyzing the impact of different network topologies on these characteristics (Pastor-Satorras et al., 2001b, Pastor-Satorras et al., 2015). Gubar et al. studied multi-strain epidemic models of heterogeneous populations on large complex networks and proposed optimal control strategies, aiding the formulation of more effective public health policies and improving early warning and response to infectious disease outbreaks (Gubar et al., 2017).

Many real-world systems can be modeled as networks, which are sets of interconnected nodes. These connections often represent channels for information transmission. A typical example is online social networks, where people pass messages or share views through their connections. When these links transmit viruses, this can be modeled as the physical transmission of viruses. However, virus transmission is a complex process, and people often choose beneficial protection strategies based on the information spread on the network. Buldyrev et al. explored the vulnerability of interconnected networks, particularly when a failure in one network spreads to another. Although they mainly focused on failure propagation, their analytical methods are valuable for understanding virus spread in multilayer networks (Buldyrev et al., 2010). Saumell-Mendiola et al. studied virus spread in interconnected multilayer networks, proposed an analytical method, and conducted numerical simulations, demonstrating the impact of multilayer network structure on transmission dynamics (Saumell-Mendiola et al., 2012). Zhan et al. proposed a nonlinear coupled complex network model based on the SIS model, showing that high prevalence rates lead to slow information decay, resulting in higher infection levels (Zhan et al., 2018). Taynitskiy et al. established a modified Susceptible-Warning-Infectious-Recovered (SWIRS) model, analyzed the optimal control problem with two control strategies (Taynitskiy et al., 2020). Sahneh et al. extended mean-field theory to epidemic transmission models in multilayer complex networks, proposed a simplified generalized epidemic mean-field (GEMF) model, and described the interaction dynamics between network layers through linearized nonlinear differential equations (Darabi Sahneh et al., 2013). Overall, multilayer network virus transmission models not only improve the realism and accuracy of modeling information transmission phenomena but also provide theoretical support for formulating effective control strategies, promoting research and application development in related fields.

This paper first introduces the significance of studying epidemic prevention measures and the evolution of epidemiological models. We then establish a single-layer SIR network model that considers node degree. Following this, experiments on breaking links between nodes and hubs reveal that severing critical links has a more pronounced effect on inhibiting virus transmission. Finally, numerical simulations on scale-free and random networks validate the accuracy of our model.

The structure of this paper is as follows: Section 2 introduces the establishment and comparative analysis of the single-layer network model; Section 3 compares and illustrates the results of virus propagation on different network structures; And finally, Section 4 presents conclusions and discussions.

2. Single-Layer SIR Network Model

In this section, we first modify the classic *SIR* model to establish a virus propagation model within a network composed of N nodes. Compared with the classic *SIR* model, we need to consider the degree of the nodes. The set of possible node states is different for different epidemic spread models. In this paper, without loss of generality, we adopt the interpretation of nodes as single individuals (Youssef et al., 2011). Let $G(V, E)$ represent an undirected graph or network, where $V = \{1, \dots, n\}$ and E is a set of links. The matrix $A = (a_{ij})_{n \times n}$ represents the adjacency matrix associated with the graph G . We also assume that the population structure is described by a scale-free network (Gubar et al., 2015). A scale-free network (SF) is a type of network topology where the degree distribution of nodes follows a power-law distribution.

In a network, nodes represent individuals, while links between nodes represent the contacts between them. Let $S_i(t)$, $I_i(t)$, and $R_i(t)$, denote the probability that individual i is in *Susceptible*, *Infected*, and *Recovered* states at time t , respectively. The *Susceptible* refers to individuals who lack immunity to the pathogen of the infectious disease and are likely to be infected upon contact. The *Infected* refers to individuals who are actively carrying the virus and may transmit it to susceptible individuals upon contact. The *Recovered* refers to individuals who have developed immunity to the virus and do not affect the transmission dynamics when interacting with others. During the epidemic, each individual i will be in any state with total probability of 1, i.e. $S_i(t) + I_i(t) + R_i(t) = 1$. This condition persists until the end of the epidemic, denoted as T .

We represent the evolution of these probabilities as a system of differential equations:

$$\begin{aligned} \frac{dS_i(t)}{dt} &= -\delta S_i(t) \sum_{j=1}^n a_{ij} I_j(t) \\ \frac{dI_i(t)}{dt} &= \delta S_i(t) \sum_{j=1}^n a_{ij} I_j(t) - \sigma I_i(t) \\ \frac{dR_i(t)}{dt} &= \sigma I_i(t) \end{aligned} \quad (1)$$

where parameter $\delta \geq 0$ is the infection rate when a susceptible node contacts an infected node, and the parameter $\sigma \geq 0$ is the recovery rate. For $(i, j) \in E$, $a_{ij} = 1$, otherwise it is equal to zero.

With the development of network science, networks in the real world are often referred to as scale-free networks (Broido et al., 2019). We consider a network generated by the algorithm designed in (Barabási et al., 1999). The pseudo-code of the algorithm is shown below.

Algorithm 1 Barabási-Albert Model Generation**Require:** N, m **Ensure:** Graph G with N nodesInitialize the network G with a small number disconnected nodes.**while** number of nodes in $G < N$ **do** Add a new node i . **for** each of the m links to be added **do** **for** each existing node j **do** Calculate the probability $p_i = \frac{k_j}{\sum_i k_i}$. **end for** Connect the new node i to an existing node j with probability p_i . **end for****end while**Calculate the connectivity distribution $P(k) \approx k^{-2}$.

At the beginning of an epidemic, most nodes in the network belong to the susceptible subgroup, with only a small fraction of the total population being infected. The remaining nodes are in the recovered subgroup. Therefore, the initial conditions of the system satisfy: $0 < S_i(0) < 1, 0 < I_i(0) < 1, R_i(0) = 1 - S_i(0) - I_i(0)$. In addition, the sum of rates of changes in the state probabilities is zero.

Theorem 1. *The system (1) gives only positive solutions for positive initial conditions.*

Proof. Starting from the differential equation $\frac{dS_i(t)}{dt} = -\delta S_i(t) \sum_{j=1}^n a_{ij} I_j(t)$, we obtain the following expression:

$$\frac{dS_i(t)}{dt} + \delta S_i(t) \sum_{j=1}^n a_{ij} I_j(t) = 0$$

By separating variables, we obtain:

$$\frac{dS_i(t)}{S_i(t)} = -\delta \sum_{j=1}^n a_{ij} I_j(t) dt$$

Solving the above equation we get:

$$S_i(t) = C e^{-\int_0^T \delta \sum_{j=1}^n a_{ij} I_j(t) dt}$$

Where C is an arbitrary constant. At time $t = 0$, we have $C = S_i(0) > 0$, thus leading to:

$$S_i(t) = S_i(0) e^{-\int_0^T \delta \sum_{j=1}^n a_{ij} I_j(t) dt}$$

This implies $S_i(t) > 0$ for all $t \in (0, T)$. Similarly, we can demonstrate that $I_i(t) \geq 0$ and $R_i(t) \geq 0$, ensuring the non-negativity of these variables throughout the analysis.

Contact does not necessarily lead to infection transmission. For each interaction between an infected individual and a susceptible individual, there is a possibility of infection transmission. This probability depends on factors such as the closeness of contact, the infectiousness of the infected member, and the susceptibility of the

susceptible member. Compared to classical compartmental models, a key modification introduced by scale-free networks is the consideration of each individual's (or node's) connectivity, which affects the probability of virus transmission to other individuals. The figure below illustrates the state transitions of each node in a virus transmission model that considers network effects.

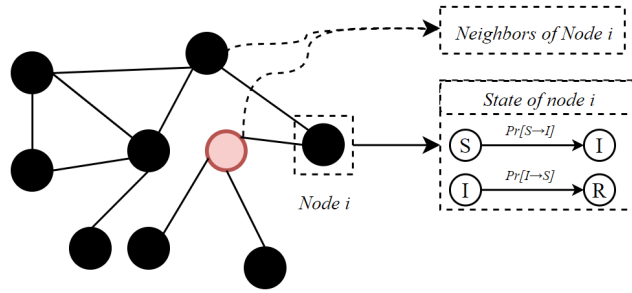


Fig. 1. Node state transition in scale-free network. Red nodes represent infected individuals, and black nodes represent susceptible individuals

Generally, the more connections a node has, the higher its probability of becoming infected. Furthermore, the probability of a node itself becoming infected depends on the number of infected individuals it is in contact with. If a node has many contacts with infected individuals, it is likely to become infected. Each infected individual tries to infect each of its susceptible neighbours at infection rate δ . Therefore, for each node, its probability of being infected is $1 - (1 - \delta)^{k_i}$, where the parameter k_i denotes the number of infected neighbor nodes of node i . Additionally, we assume that once infected, a node recovers at a fixed recovery rate, transitioning to the recovered state. Thus, the probability of a node transitioning from the infected state to the recovered state is σ .

3. Numerical Simulation

After establishing the probabilities governing state transitions for each node, we first initialize the system. This setup includes constructing the network topology and assigning an initial state to each node. Once initialized, the system can proceed with iterative updates to each node's state over each time moment t .

At each time moment t , we evaluate the status of every node in the network. For susceptible nodes, we identify any neighboring nodes in an infected state and apply the predefined transmission probability to assess whether they become infected. Conversely, if a node is infected, we apply the recovery rate to determine whether it transitions back to a recovered state. By recording each node's state at every time step, we construct an infection curve that reflects the dynamics of disease spread within the network. The algorithm for implementing these state transitions is outlined in the pseudocode below.

Algorithm 2 Node State Transition

Require: Network structure, initial node states, transition probabilities, recovery rates**Ensure:** Infection curve

Initialization: Build the network structure and set the initial state of each node.

for each moment t **do** **for** each node i **do** **if** node i is susceptible **then** Find infected neighbor nodes of i . Determine the next state of i using the defined probabilities. **else if** node i is infected **then** Determine the next state of i using the defined recovery rate. **end if** **end for**

Count the state of each node in the network to obtain the infection curve.

end for

3.1. Propagation on the Scale-Free Network

Within scale-free networks, "hub", "remote", and "normal" constitute three distinct node classifications that are commonly utilized to depict the topological features of nodes within the network context. Specifically, a "hub" refers to a node possessing an extremely high degree of connectivity and assumes a critical central role in the network. In contrast, a "remote" node features a remarkably low degree and generally connects to merely a few other nodes in the network. Meanwhile, a "normal" node has a moderate level of connectivity and belongs neither to the category of hub nodes nor that of remote nodes. Based on the degree of each node, we categorize nodes into three distinct groups:

- A node i is classified as a **hub** if its degree k_i satisfies $k_i \geq k_{p1}$. Where k_{p1} represents the $p1$ -th quantile of the degree distribution. In this study, $p1 = 0.95$, corresponding to the top 5% of high-connected nodes.
- A node i is classified as a **remote** if its degree k_i satisfies $k_i \leq k_{p2}$. Where $p2 = 0.05$, representing the bottom 5% of low-connected nodes.
- A node i is classified as a **normal** if its degree k_i lies in the range $k_{p2} < k_i < k_{p1}$.

Regarding the initial values of the system, we assume that at the beginning of the epidemic, the number of infected individuals is small. This configuration indicates that the initial state comprises two infected individuals and zero recovered individuals, with the rest being susceptible. The total population size is set to $N = 5000$. We set the infection rate of the virus $\delta = 0.3$ and the recovery rate $\sigma = 0.1$. The following figure compares the results of the virus transmission model with and without considering a scale-free (SF) network.

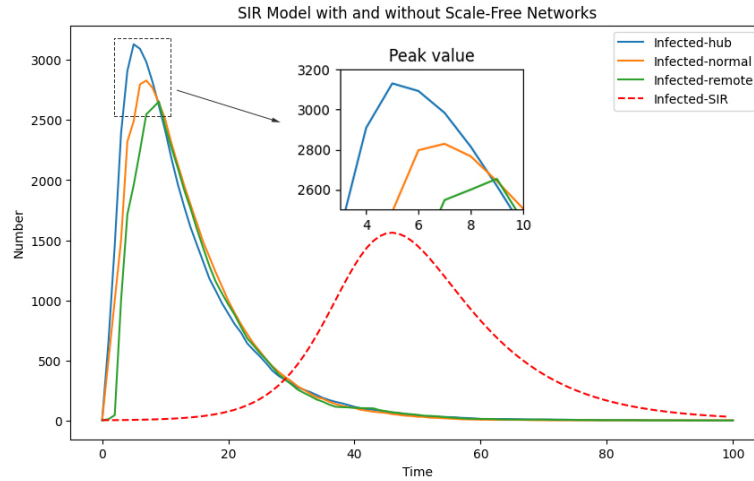


Fig. 2. SIR model with and without Scale-Free networks. "Infected-hubs", "Infected-remote" and "Infected-normal" denotes the simulation result of selecting hub, remote and normal nodes respectively in the scale-free network as the initial infectors. And "Infected-SIR" denotes that the classical compartmentalized SIR model randomly selects nodes for infection without considering the SF network. The inset shows the detailed results of the peak

To clearly illustrate the importance of network node selection, the table below presents the numerical results of the simulation.

Table 1. Comparison results of SIR model with and without Scale-Free networks

Different initial states		Peak number	Time to reach peak number
With SF Network	Infected-hub	3131	5
	Infected-normal	2829	7
	Infected-remote	2654	9
Without SF Network	Infected-SIR	1563	46

The table shows the peak number of infections and the time required to reach the peak under different initial conditions. Combining Figure 2 and Table 1, we find that in the presence of an SF network, when infections are concentrated in the hub nodes (Infected-hub), the peak number of infections is the highest, at 3131 individuals, and it occurs the fastest, in just 5 days. When infections are in random nodes (Infected-normal), the peak number of infections is 2829, requiring 7 days. When infections are in remote nodes (Infected-remote), the peak number of infections is 2654, requiring 9 days. In the absence of an SF network (Infected-SIR), the peak number of infections is the lowest, at only 1563, and the time to peak is the longest, at 46 days. These values indicate that in the presence of an SF network, infections concentrated in hub nodes result in faster and more widespread infection, whereas in the absence of an SF network, infection spreads more slowly and peaks at a lower number.

To facilitate a more intuitive study of the impact of network structures on virus transmission models, we set the total number of nodes to 50. The figure below shows the constructed SF network structure.

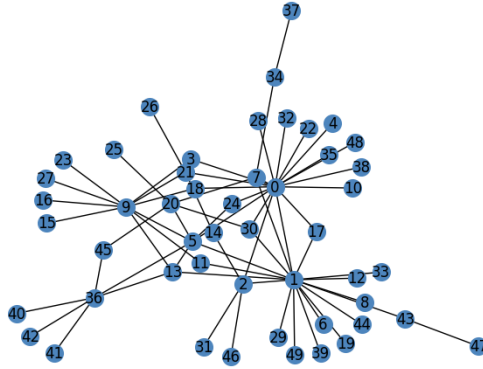


Fig. 3. The network structure of scale-free network with 50 nodes

In order to study the impact of network properties on virus propagation. We classify each node according to its degree and its distance to the hubs and study how these classifications affect virus transmission. The figure below shows the degree and distance distribution of the network structure in Figure 3.

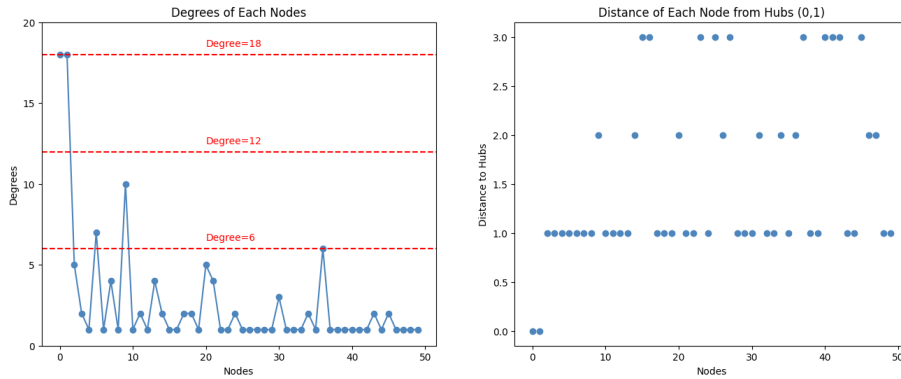


Fig. 4. The network structure of Figure 3. The left side shows the node degree distribution of the network structure and the right side shows the distance of each node from the hubs

Based on the degree distribution of the network nodes, we divide the nodes into three categories: 0-6, 6-12, and 12-18(hubs). The distances to the hubs are categorized as 0 (hubs), 1, 2, and 3. For better consideration of the network structure, we use the speed as an indicator of epidemic process. Here, speed is defined as the ratio of the peak value of the time to reach the peak, $Speed = \frac{Peak\ value}{Time\ to\ reach\ the\ peak}$, which represents the speed to reach the peak. First, we randomly select two nodes in each

category as the initial infected nodes based on the degree and distance classification of the SF network. Then, we conduct numerical simulation experiments, setting the number of experiments to 50. The infection rate and cure rate are set to 0.3 and 0.1, respectively. We use histograms to present the experimental results. In histograms, "frequency" represents the number of occurrences of a calculated speed in different bins under specific conditions.

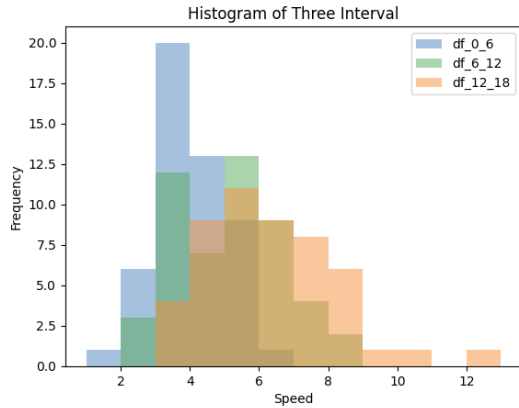


Fig. 5. Histograms of speed for three degree intervals. df_{0_6} , df_{6_12} , df_{12_18} denote different intervals of degree classification respectively

In the figure above, as the degree increases, the average speeds for the three intervals are 3.89, 5.04, and 6.16(hubs), respectively. The results indicate that if nodes with higher degrees are chosen as the initial infectors, the average spread of the virus will be faster. Similarly, we set the number of experiments to 50. The infection rate and cure rate are set to 0.3 and 0.1, respectively. However selecting initial infected nodes based on their distance to the hubs.

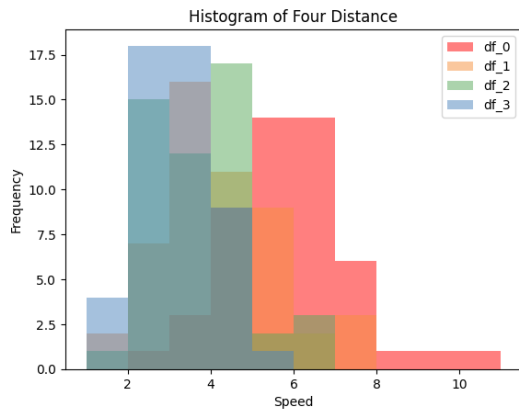


Fig. 6. Histograms of speed for four distances. df_0 , df_1 , df_2 , df_3 denote different intervals of distance classification respectively

In the figure above, as the distance from the hubs increases, the average speeds corresponding to the four distances are 5.83 (hubs), 4.08, 3.87, and 3.07, respectively. The results show that if a node close to the hub is chosen as the source of infection, the average spread of the virus will be faster. We further classify the nodes into important nodes, normal nodes, and remote nodes. The pseudocode below shows the specific steps for classifying the nodes.

Algorithm 3 Node Classification

Require: Network graph G , Hub nodes

Ensure: Classification of nodes

Get the degree and distance of the network nodes.

for each node i in G **do**

 Calculate the distance of node i to the nearest hub.

end for

for each node i in G **do**

if distance of i to hub is 1 and degree of $i > 1$ **then**

 Classify node i as **Important**.

else if distance of i to hub is larger than 1 and degree of $i \neq 1$ **then**

 Classify node i as **Normal**.

else if degree of $i == 1$ **then**

 Classify node i as **Remote**.

end if

end for

The reason for this grouping is that if a node is close to the hubs, it is considered an important node. These nodes are sorted by their degree, effectively ranking them by their importance. Cutting off the link between this important node and the hubs effectively increases the distance to the hubs and reduces the cost of controlling the epidemic. The figure below shows the network structure after breaking the links according to the above algorithm.

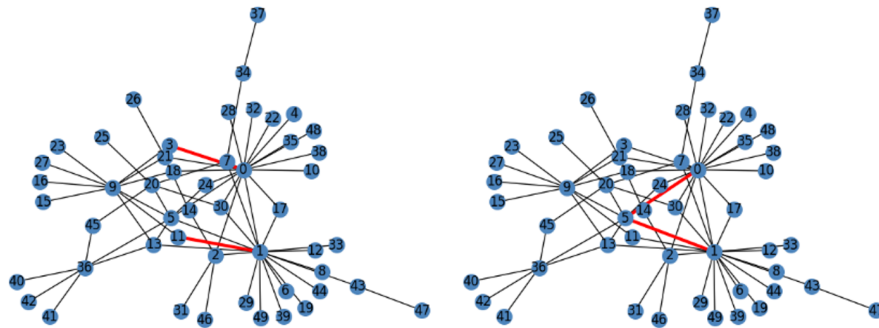


Fig. 7. Disconnect the SF network node link. Red lines indicate broken links. According to the classification basis above, the left side is for disconnecting normal nodes and the right side is for disconnecting important nodes

After breaking the links, we set the number of experiments to 50. The infection rate and cure rate are set to 0.3 and 0.1, respectively. The results are shown below.

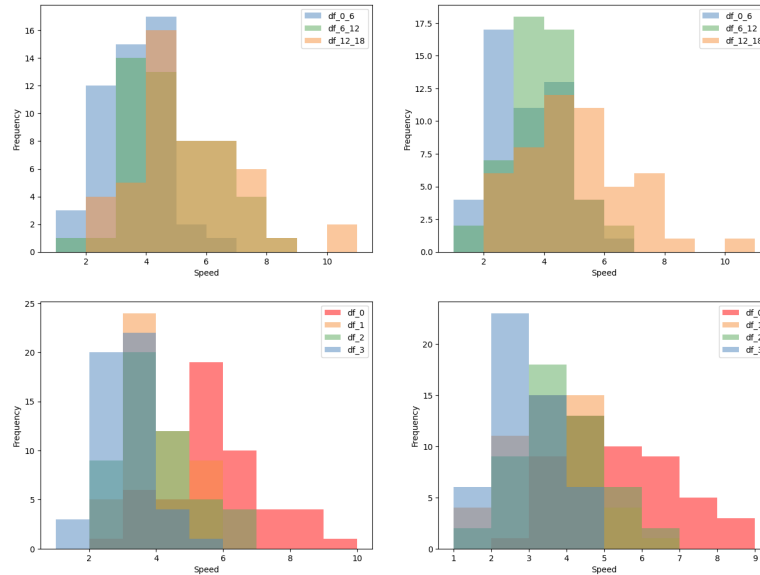


Fig. 8. Histogram of speed distribution after disconnecting links. The left half shows the histogram of the speed when disconnecting the links of normal nodes and hubs. The right half shows the histogram of the speed when disconnecting the links of important nodes and hubs

Corresponding to the figure above, the table below presents the average speed under various disconnection conditions.

Table 2. Average speed of reaching peak under different disconnection conditions

Disconnect condition	Average Speed						
	Degree interval			Distance to hubs			
	0-6	6-12	12-18 (hubs)	0 (hubs)	1	2	3
none	3.89	5.04	6.16	5.83	4.08	3.87	3.07
important	3.36	3.86	4.99	5.34	3.59	3.72	2.93
normal	3.51	4.84	5.25	5.64	3.88	3.78	3.06

In the table above, "none" represents the original network structure. The data illustrate the average speed of virus spread under various disconnection conditions and for different intervals of initially infected individuals. The results indicate that breaking normal links has a positive impact on virus transmission. In addition, breaking important links has a greater effect on inhibiting virus transmission compared to breaking normal links. Therefore, when controlling an epidemic, to control costs, we can choose to break "important" links without isolating all nodes.

3.2. Propagation on the Random Network

To conduct an in-depth and precise investigation into virus transmission characteristics across various network structures and to avoid superficial or generalized conclusions, we used a random network as a control in our experiments. In this network, connections between nodes form randomly according to a given probabil-

ity, without any preference for specific nodes or topological patterns. The connection probability remains constant, lending randomness and unpredictability to node connections. By simulating and analyzing the virus transmission process within a random network and comparing it to other network structures, we can gain a more comprehensive understanding of how network structure fundamentally influences virus transmission mechanisms.

Similar to the scale-free (SF) network, we used identical initial conditions. In a random network, two initial infected nodes were randomly selected, with all other nodes set as susceptible. For the network configuration, we set the number of nodes to 50 and the connection probability between nodes to 0.2. The structure of a random network is illustrated in the figure below.

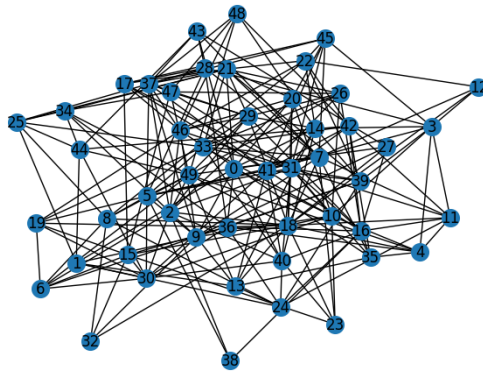


Fig. 9. T structure of a random network with 50 nodes

To investigate the effects of different parameters on different networks, we divided infection rates and cure rates into five groups. The first group is the reference group, with infection and cure rates set to 0.3 and 0.1, respectively. In the second group, we reduced both values to 0.2 and 0.05. The third group only increases the cure rate to 0.2 while keeping the infection rate constant at 0.3. The fourth group increases the infection rate to 0.4 while keeping the cure rate unchanged. In the final group, both infection and cure rates are increased to 0.4 and 0.2, respectively.

In order to study the impact of selecting different initial infection nodes on virus spread, we categorized each network's nodes based on degree into three types: Hub (high-degree nodes), Normal (medium-degree nodes), and Remote (low-degree nodes). In each experiment, the initial infection nodes consist of two randomly selected nodes from one of these categories.

Remark 1. In each network, node classification is based on a simple degree ranking to obtain these three types of nodes. If only one high-degree node exists in the network, which is the Hub, however we need to set two initial infection nodes, we will select the node with the highest degree in the next category (Normal).

After initializing the values and setting up the network, we adopt propagation speed as the measurement metric. Here, propagation speed refers to the speed at which the virus reaches its peak value. The larger the speed value is, the more

rapidly the virus spreads within the network. The following table shows the average value obtained from 50 experiments.

Table 3. Average speed of reaching peak value on different networks

Networks	Parameter		Remote(Average)	Normal(Average)	Hub(Average)
	δ	σ	speed to peak	speed to peak	speed to peak
Scale - Free	0.3	0.1	1.67562724	2.143712575	2.74801061
	0.2	0.05	1.26873385	1.366790582	1.922580645
	0.3	0.2	1.462427746	1.821637427	3.015564202
	0.4	0.1	2.421052632	2.80349345	3.478134111
	0.4	0.2	2.12849162	2.612582781	3.683127572
Random	0.3	0.1	7.805970149	8.298804781	8.846808511
	0.2	0.05	6.105413105	6.534328358	7.476190476
	0.3	0.2	6.952755906	7.948051948	8.558685446
	0.4	0.1	9.452586207	9.903225806	10.9009901
	0.4	0.2	8.745454545	9.647058824	9.862244898

From the table presented above, it can be clearly observed that each set of parameters exerts a significant influence on both the peak infection level and the network transmission speed. When the infection and recovery rates are reduced, it is typically noted that the transmission speed is generally slowed down, and the peak time is correspondingly delayed. Conversely, when these rates are increased, it leads to faster transmission speeds and higher peak infection levels. In order to more effectively illustrate these distinct differences, the figure provided below displays the transmission speed of the virus across different networks under a variety of parameter settings. It provides valuable insights for further analysis and research in the related field, enabling a more detailed exploration of the underlying mechanisms and potential strategies for disease control and prevention.

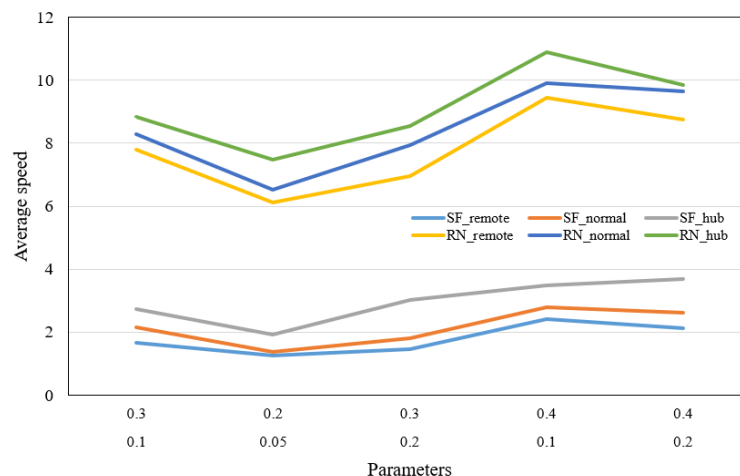


Fig. 10. Average speed of reaching peak value on different networks

The figure above clearly demonstrates significant differences in virus transmission behaviors between scale-free and random networks. Compared to scale-free networks, random networks exhibit faster transmission speeds and higher peak infection levels, indicating that network topology plays a crucial role in transmission dynamics. Hub nodes with the highest connectivity result in faster transmission speeds compared to remote nodes, which show lower peak levels and slower transmission rates. This suggests that targeting highly connected nodes could be a more effective strategy in network control measures to reduce transmission potential.

4. Conclusions and Discussion

The research clearly demonstrates that network topology significantly influences epidemic processes. In scale-free networks, the degree distribution of nodes affects the spread of infections. Hub nodes play a crucial role, with infections concentrated in them resulting in faster and more widespread spread. In contrast, random networks exhibit different transmission characteristics, generally having faster transmission speeds and higher peak infection levels.

The degree and distance of nodes from hubs are important factors. Nodes with higher degrees or closer to hubs have a higher probability of transmitting infections faster. This understanding can be used to develop more effective control strategies, such as targeting highly connected nodes or those close to hubs.

The single-layer SIR network model provides a useful framework for understanding epidemic spread in networks. The numerical simulations based on this model offer insights into how different network structures and node characteristics impact the dynamics of disease spread. Future research could explore more complex network models and consider additional factors such as human behavior and multiple strains of diseases to further enhance our understanding of epidemic processes in networks.

References

- Barabási, A. L., Albert, R. (1999). *Emergence of scaling in random networks*. *Science*, **286**(5439), 509–512.
- Bloom, D. E., Cadarette, D. (2019). *Infectious disease threats in the twenty-first century: strengthening the global response*. *Frontiers in Immunology*, **10**, 549.
- Brauer, F. (2008). *Compartmental models in epidemiology*. In *Mathematical Epidemiology* (pp. 19–79).
- Broidó, A. D., Clauset, A. (2019). *Scale-free networks are rare*. *Nature Communications*, **10**(1), 1017.
- Buldyrev, S. V., Parshani, R., Paul, G., Stanley, H. E., and Havlin, S. (2010). *Catastrophic cascade of failures in interdependent networks*. *Nature*, **464**(7291), 1025–1028.
- Darabi Sahneh, F., Scoglio, C., Van Mieghem, P. (2013). *Generalized epidemic mean-field model for spreading processes over multilayer complex networks*. *IEEE/ACM Transactions on Networking*, **21**(5), 1609–1620. <https://doi.org/10.1109/TNET.2013.2239658>
- Fu, X., Small, M., Walker, D. M., Zhang, H. (2008). *Epidemic dynamics on scale-free networks with piecewise linear infectivity and immunization*. *Physical Review E*, **77**(3), 036113. <https://doi.org/10.1103/PhysRevE.77.036113>
- Gubar, E., Kumacheva, S., Zhitkova, E., Porokhnyavaya, O. (2015). *Propagation of information over the network of taxpayers in the model of tax auditing*. In 2015 International Conference 'Stability and Control Processes' in Memory of V.I. Zubov (SCP) (pp. 244–247). St. Petersburg, IEEE. <https://doi.org/10.1109/SCP.2015.7342116>
- Gubar, E., Zhu, Q., Taynitskiy, V. (2017). *Optimal control of multi-strain epidemic processes in complex networks*. In L. Duan, A. Sanjab, H. Li, X. Chen, D. Materassi, and R. Elazouzi (Eds.), *Game Theory for Networks* (pp. 108–117). Cham: Springer International Publishing.
- Kermack, W. O., McKendrick, A. G. (1927). *A contribution to the mathematical theory of epidemics*. *Proceedings of the Royal Society of London. Series A, Containing Papers of a Mathematical and Physical Character*, **115**(772), 700–721.
- Pastor-Satorras, R., Castellano, C., Van Mieghem, P., Vespignani, A. (2015). *Epidemic processes in complex networks*. *Reviews of Modern Physics*, **87**(3), 925–979.
- Pastor-Satorras, R., Vespignani, A. (2001). *Epidemic spreading in scale-free networks*. *Physical Review Letters*, **86**(14), 3200–3203. <https://doi.org/10.1103/PhysRevLett.86.3200>
- Pastor-Satorras, R., Vespignani, A. (2001). *Epidemic dynamics and endemic states in complex networks*. *Physical Review E*, **63**(6), 066117.
- Payne, J. F. (1893). *History of epidemiology in England*. *Lancet*, **2**, 1293.
- Saumell-Mendiola, A., Serrano, M. Á., and Boguná, M. (2012). *Epidemic spreading on interconnected networks*. *Physical Review E-Statistical, Nonlinear, and Soft Matter Physics*, **86**(2), 026106.
- Tamerius, J., Nelson, M. I., Zhou, S. Z., Viboud, C., Miller, M. A., Alonso, W. J. (2011). *Global influenza seasonality: reconciling patterns across temperate and tropical regions*. *Environmental Health Perspectives*, **119**(4), 439–445.
- Taynitskiy, V., Gubar, E., Fedyanin, D., Petrov, I., Zhu, Q. (2020). *Optimal control of joint multi-virus infection and information spreading*. arXiv, Jul. 19, 2020. Accessed: May 31, 2024. [Online]. <http://arxiv.org/abs/2007.09745>.
- Youssef, M., Scoglio, C. (2011). *An individual-based approach to SIR epidemics in contact networks*. *Journal of Theoretical Biology*, **283**(1), 136–144. <https://doi.org/10.1016/j.jtbi.2011.05.029>
- Zhan, X., Chuang, L., Ge, Z., Zi-Ke, Z., Gui-Quan, S., Jonathan, J. H., Zhu, Zhen J. (2018). *Coupling dynamics of epidemic spreading and information diffusion on complex networks*. *Applied Mathematics and Computation*, **332**, 437–448. <https://doi.org/https://doi.org/10.1016/j.amc.2018.03.050>